We are IntechOpen, the world's leading publisher of Open Access books Built by scientists, for scientists

6,900
Open access books available

185,000
International authors and editors

200M
Downloads

Our authors are among the

154
Countries delivered to

TOP 1%
most cited scientists

12.2%
Contributors from top 500 universities



WEB OF SCIENCE™

Selection of our books indexed in the Book Citation Index in Web of Science™ Core Collection (BKCI)

Interested in publishing with us?
Contact book.department@intechopen.com

Numbers displayed above are based on latest data collected.
For more information visit www.intechopen.com



Chapter

Stoichiometric and Nonstoichiometric Compounds

Paras Dubey and Netram Kaurav

Abstract

This chapter gives a general overview of synthesis and recent development of nickel oxide as a nonstoichiometric compound. We establish the synthesis chemistry of nickel oxide as a nonstoichiometric material, and hence successively introduce definitions and classifications of nonstoichiometric compounds as well as their point defects. The samples of nonstoichiometric nickel oxide are synthesized by thermal decomposition method. The nonstoichiometry of samples was then studied chemically by iodometric titration, and the results are further corroborated by excess oxygen obtained from the thermo-gravimetric analysis (TGA). X-ray diffraction (XRD) and Fourier transformed infrared (FTIR) techniques are used to analyze structural phase of nonstoichiometric nickel oxide. The change in oxidation state of nickel was studied by X-ray photoelectron spectroscopy (XPS) analysis. The shift in antiferromagnetic ordering and transition temperature due to nonstoichiometry is studied by magnetic and specific heat capacity analysis.

Keywords: nonstoichiometry, defect study, nickel oxide, thermo-gravimetrical analysis, iodometric titrations

1. Introduction

In solid-state chemistry, the study of compound has been expanded to the crystal structure level. The law of definite proportions, the law of constant composition, and the law of conservation of mass state that a chemical compound always contains exactly the same proportion of elements by mass. All chemical compounds obeying these laws are called as stoichiometric compounds. While nonstoichiometric compounds are the chemical compounds deviated from stoichiometry, namely their elemental composition cannot be represented by a ratio of well-defined natural numbers, and therefore violate the law of definite proportions, hence a nonstoichiometric compound is a type of special solid-state compound with definite structure and thermodynamic characteristics, which differs from its stoichiometric counterpart and a mixture. Due to defect structure in a continuous manner, these compounds are different with stoichiometric compounds. Beside some unusual information on solid-state chemistry, stability, and dynamics can be explore through their structure and characteristic. These nonstoichiometric compounds exhibit different properties such as conductivity, magnetism, catalytic nature, color, and other unique solid-state properties, which have important technological applications.

Experimental and calculated results demonstrate that the migration of anion and cation vacancies and the formation of insulating vacancy clusters near the vicinity of the interface are the fundamental switching mechanism [1]. The enhancement in photoconduction under below-band gap light illumination is attributed to the transition from defect levels (e.g., oxygen vacancies) [2]. The unique properties are determined by their solid phase composition, thermodynamic properties, and crystal defect structure. These properties depend upon the structure and phase of the crystal; hence, the unit cell parameter plays an important role in nonstoichiometric compound, which varies in a definite manner. The microscopic structural and macroscopic thermodynamical properties also vary with phase and unit cell parameters. The X-ray diffraction study reveals that as the composition of the nonstoichiometric compound changes, the cell parameter and other property continuously changes, which is different from crystalline stoichiometric compound. Hence, X-ray diffraction and chemical analysis are important tools to investigate the nonstoichiometry [2]. The lattice defect can be analyzed by their different properties [2]. Hence, nonstoichiometry plays very important role in the solid compounds of transition metals and becoming a challenge and new opportunity in chemistry. Therefore, study of the nonstoichiometric compounds has become an interesting field in solid-state chemistry and defect chemistry.

There are significant structural changes that are seen in nonstoichiometric compounds. The phase of matter changes as external conditions such as pressure, temperature, or chemical composition are varied. Due to sudden change in these external thermodynamical conditions, the crystalline structure also changes. Thus, an abrupt change in thermodynamical conditions, such as specific volume, entropy, or specific heat, also changes the derivatives of free energy. Therefore, these parameters can be used as a helpful indicator of phase transitions. The abrupt changes can identify them as driven by a pseudo phase transition that is a result of a sharp switch of predominant defect species [3]. The defect that is introduced by sudden change in conditions, changes the physical properties of a material. It is quite different from the abrupt variation in physical properties that arises from symmetry or ordering change in a conventional phase transition. Therefore, according to the conventional classification, a defective state of a material cannot be labeled as a distinct physical phase compared with the perfect one.

In this chapter, we tried to understand the effect of change in stoichiometry of nickel oxide compound. We have prepared the samples of nickel oxide with thermal decomposition method. The samples were analyzed by different characterized methods and found to nonstoichiometric. The effect of nonstiochiometry on oxidation state, bonding between oxygen and nickel, magnetic property, specific heat, and structural property were studied.

2. Classification and point defect formation in nonstoichiometric compounds

The compounds with uniform physical phase in which unit cell parameters vary with its composition in a continuous manner are nonstoichiometric. The free energy of such compounds is function of composition and temperature of the system. The chemical potential depends on the composition of solid, and due to microscopic and macroscopic characteristics, the structural and thermodynamical property changes. Different parameters of crystallography cell, obtained by X-ray diffraction analysis, change due to nonstoichiometry. This parameter continuously varies with its composition [3].

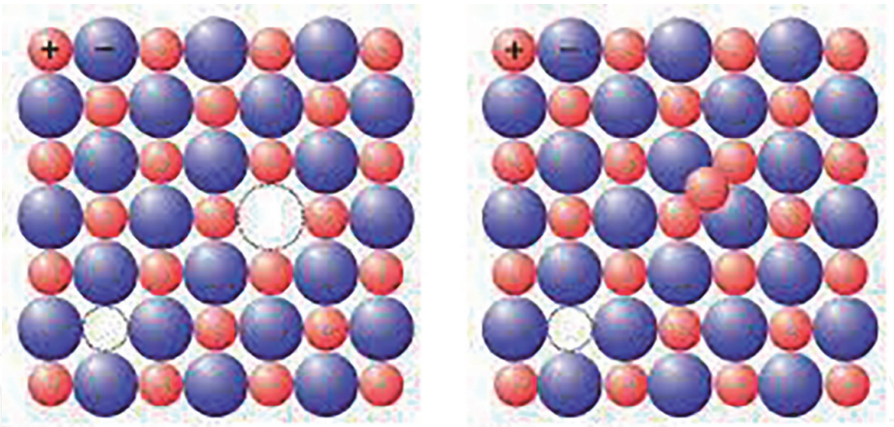


Figure 1.
Schottky and Frenkel defects.

Element composition is the main criteria to classify the nonstoichiometric compounds. These compounds exist only in the condensed state. Transition metal oxides are generally nonstoichiometric, some nitrides and sulfides also comes under such category [4–6]. Most nonstoichiometric compounds have compositions that are close to those of stoichiometric compounds and can be expressed by formulas such as WO_{3-x}, $Co_{1-x}O$, $Zn_{1+x}O$, and $Ni_{1-x}O$, in which x is a positive quantity much smaller than 1. In the first case, an oxygen vacancy would be formed, and in some cases, there is metallic deficiency that is seen. Due to deviation from stoichiometric composition, it would result in the formation of some lattice imperfections. Hence, in some nonstoichiometric compounds, there are anionic vacancies and in some, there are cationic vacancies. These vacancies are formed due to defects in the lattice structures of crystalline substances, such as the absence of ions from sites that would normally be occupied. The crystallographic point defects are the main defects in which interstitial atoms and vacancies resulting from excess or deficiency of a component element. Point defects are an important cause of formation of the nonstoichiometric compounds. There are two main point defects in nonstoichiometric compounds namely Frenkel defect and Schottky defect. The Frenkel defect explains a defect in the molecule, where an atom or ion (normally, the cation) leaves its own lattice site vacant and instead occupies a normally vacant site, while the Schottky defect forms when vacancies are created when oppositely charged ions leave their lattice sites. Formation of theses vacancies in stoichiometric system helps in maintaining an overall neutral charge in the ionic solid. These created vacancies are filled by the movement of surrounding atoms, due to which new vacancies are formed. The formation of defects in the crystal will lead to a decrease in the density of the crystal or metal. This can be understood by **Figure 1**.

3. Nonstoichiometry in nickel oxide

Nickel oxide is an antiferromagnetic [7] and Mott-Hubbard insulator [7]. Nickel oxide (NiO) has been among some of the transition metal oxide, which is most thoroughly studied by the researchers. It can be easily synthesized and is very low in preparation cost, the nature of this material is such that it has low toxicity and it is environmental friendly. These properties of nickel oxide attracted considerable interest of the researchers. Due to its versatility, nickel oxide is useful in number of applications, such as transparent conductive film [8], chemical sensors [9], and

resistive random access memory [10]. The positive electrode in batteries [11] and in quantum dot light emitting devices as a hole transport layer [12] are some of the very latest and important applications of nickel oxide material. The condition of synthesis of the material plays very important role in the applications. If the condition of sample preparation changes, then the oxygen content of the sample also changes, and NiO of different stoichiometry ($Ni_{1-\delta}O$) can be obtained. In such samples, the composition ratios between nickel and oxygen are not exactly 1:1. Because of excess oxygen and vacancies on Ni site, nickel oxide thus becomes a p-type metal-deficit semiconductor [8]. The findings of investigations done by authors suggest that Ni vacancy is the most dominant point defect present in the system, rather than oxygen interstitial [13, 14]. The distribution of vacancy over a particular volume is an important issue. Due to difference in the nature of surface and bulk, the defect formation and hence distribution of vacancy will be different. The charge transport in NiO, as in other transition metal oxides, is of the thermally activated hopping type, and electron holes are localized at cation lattice sites. The nature of defect clusters and complexes in metal-deficit NiO, as well as the role of specific impurities, influence remarkably the different characteristic properties of nonstoichiometric NiO. This specific vacancy distribution has its strong effect on the overall electrical [15], optical [16], and thermal [17] properties, depending strongly on its stoichiometry.

The main reason for changes in properties could be the excess oxygen present in the samples. This excess oxygen also changes the oxidation state of nickel, which produces a vacancy at the metal side to produce cation vacant nickel oxide. As the temperature of sintering of precursor increases, the excess of oxygen decreases. Due to increase in the excess of oxygen, densities of nickel oxide and activation energy of electrical conductivity decrease, but the lattice parameter of such samples is unaffected [18]. The diffusion of vacancies to the crystal surface is the main reason for the decrease in vacancies [19].

NiO adopts the NaCl structure, with octahedral Ni(II) and O^{2-} sites. The conceptually simple structure is commonly known as the rock salt structure. Like many other binary metal oxides, the nonstoichiometry is accompanied by a color change, with the stoichiometrically correct NiO being green and the nonstoichiometric NiO being black. Bulk material of NiO has a cubical crystal structure, and it shows antiferromagnetic behavior below Neel temperature, and above it, the structure is transformed into a cubic one with paramagnetic behavior [20]. The change in the particle size is attributed to the excess oxygen present in nonstoichiometric nickel oxide. Scientist suggested that due to the change in oxygen content of the sample, the complexity of the disordered arrangement, volume distribution, and random orientation of the magnetization vector changes; hence, thermal, optical, electrical, magnetic, and many other properties of sample change. Due to the change in the particle size of antiferromagnetic materials sintered at different temperatures, the surface to volume ratio becomes sufficiently large. Because of their large surface area, the existing uncompensated spins give a nonzero net magnetic moment.

4. Synthesis of nonstoichiometric nickel oxide

Preparation of compound plays an important role in its characteristic properties. Nonstoichiometric compounds, whose composition and structure are known, are very important as they have unique optical, electrical, magnetic, thermal, and mechanical properties. The selection of precursor for design and tailoring the materials of different stoichiometry for desirable performance is of great interest. By means of effective and precise control of the composition, defect, and structure, the

nonstoichiometry can be created. Depending on the conditions of preparation, the sintering temperature, in particular, NiO samples of various surface areas, colors, and degrees of nonstoichiometry can be prepared. Nickel oxide can easily be prepared via several methods, including chemical route, evaporation [12], sputtering [8], chemical deposition [21], oxidation of nickel [22], sol-gel method [23], and thermal decomposition [24]. Thermal decomposition method is a typical powder preparation method, which is simple, low-cost, and fast endothermic process.

Nonstoichiometric nickel oxide was obtained by thermal decomposition of nickel nitrate hexahydrate [25]. Typically, about 5 g $Ni(NO_3)_2.6H_2O$ was decomposed thermally in open air for 3 hours at 400°C to produce nickel oxide sample with a particular content of oxygen ($Ni_{1-\delta}O$). The product thus obtained was pure and contains no other mixture. This exothermic reaction is noncatalytic and does not require any other substance to initiate the reaction. The output material obtained by breaking down the precursor is nickel oxide and gaseous parts, which are escaped from the system freely. The decomposition mechanism of this process takes the minimum time-temperature condition. This sample was denoted as NiO400. Similarly, seven other samples were prepared at 500, 600, 700, 800, 900, 1000, and 1100°C. They were denoted NiO500, NiO600, NiO700, NiO800, NiO900, NiO1000, and NiO1100, respectively.

5. Characterization of nonstoichiometric nickel oxide

The study of compositions, substance phase, and defect are main parameters to characterize nonstoichiometric compounds. The effect of nonstoichiometry on composition, structure, and other properties is studied while characterizing these types of solids. These properties highly depend on the defects in the crystal. In the present study, composition can be determined by means of chemical analysis by iodometric titration, which was corroborated by thermo-gravimetric analysis (TGA). Phase and structure can be examined through X-ray diffraction, XPS analyses, and relationship of the composition, structure, and properties can be detected using FTIR, magnetic measurement, and specific heat measurement. So, we can categorically confirm that the nickel oxide is a nonstoichiometric compound rather than a stoichiometric compound. Furthermore, this FTIR also confirms the bonding of oxygen with metal ions, and shift in the FTIR peaks indicates change in stoichiometry of the as prepared samples.

Oxidation sate along with chemical nature and binding state were analyzed by X-ray Photoelectron Spectroscopy (XPS). This method is a surface analytical method, hence all the properties that change with composition were studied by this method. The behavior of transition temperature with change in stoichiometry was studied by temperature dependence of magnetic susceptibility (c) and heat capacity (Cp).

5.1 Structure determination of nonstoichiometric nickel oxide

To confirm the phase structure of polycrystalline powder sample, X-ray diffraction technique is one of the most important methods. This method can be used for the determination of the phase structure and unit cell parameters. The XRD measurements of the nonstoichiometric nickel oxide samples are conducted with the help of Bruker D8 Advance X-ray diffractometer. Cu Kα radiation (0.154 nm) is used for the analysis, and measurements were done in the angle ranging 10–90°. Silicon strip technology is used to detect the scattered X-ray radiations.

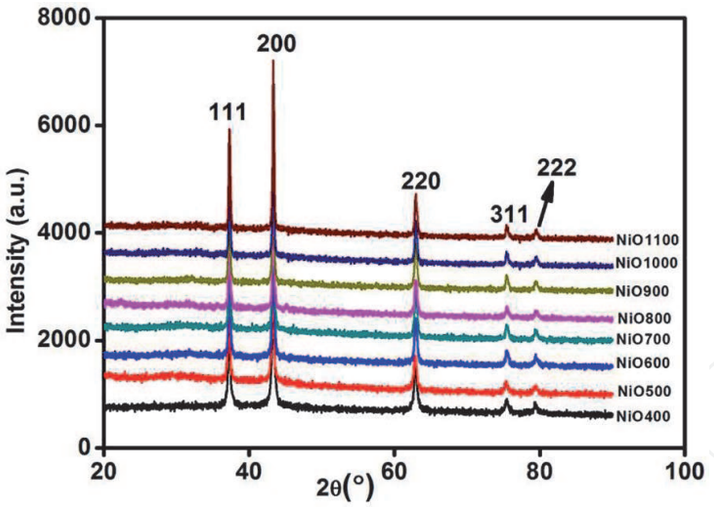


Figure 2.
X-ray diffraction patterns of different nonstoichiometric samples.

Intensity (%)	2θ	$Sin^2\ \theta$	$h^2 + k^2 + l^2$	C	(hkl)	a(Å)	ā(Å)
61.69	37.279	0.1022	3	0.034	(111)	4.1772	4.1775
100	43.472	0.1365	4	0.034	(200)	4.1727	
44.83	62.901	0.2722	8	0.034	(220)	4.1772	
15.68	75.416	0.3741	11	0.034	(311)	4.1772	

Table 1.
Crystallographic data using analytical analysis for NiO samples.

XRD analysis was employed to investigate the crystallinity and purity of the solid product obtained by thermal conversion in air of the polycrystalline compounds. **Figure 2** shows XRD patterns of $Ni_{1-\delta}O$ samples, NiO400, NiO500, NiO700, NiO1100 and NiO600, NiO800, NiO900, and NiO1000. XRD peaks match well with the standard XRD of with no other impurity peaks, showing that these samples were of a single phase in nature in each of them. The XRD data show the presence of the characteristic peaks for NiO at 2θ in the range of 10–90°, in accordance with JCPDF File 47-1049. The lattice parameters were obtained from the following relationship analytically: $\sin 2\theta = C\ (h^2 + k^2 + l^2)$, where $C = \lambda^2/4a^2$. The results of the X-ray structural analysis are given in **Table 1**.

On comparing peaks obtained in X-ray analysis with standard JCPDF File 47-1049, we conclude that the precursor salt is transformed to NiO. Hence, data from analytical and structural analysis corroborate with the experimental data. This indicates that the NiO obtained by thermal conversion in air of the poly-nuclear coordination compounds is face-centered-cubic phase, also known as the bunsenite structure (lattice constant a of cubic unit cell, 0.4177 nm). Phase of the NiO prepared by thermal decomposition method is stable, as no other peaks were seen in the structural analysis.

Further, Sherrer formula: $L = k\lambda/\beta\cos(\theta)$ is used to calculate the mean crystallite size of the NiO sample where L is the crystallite size, k is the Sherrer constant, usually taken as 0.89, λ is the wavelength of the X-ray radiation (0.154056 nm for Cu Kα), and β is the full width at half maximum (FWHM) of diffraction peak measured at 2θ.

The deduced values of crystallite size of the analyzed NiO samples are reported in **Table 2**, which indicates that as the sintering temperature of precursor increases the crystallite size of NiO changes.

Compounds	a (Å)	V (Å^3)	Rf factor	Bregg's R-factor	R_p	R_{wp}	R_e	χ^2	*L* (nm)
NiO (400°C)	4.176	72.82	2.39	3.94	24	16.7	14.9	1.26	240
NiO (500°C)	4.174	72.74	4.44	4.33	29	19.6	16.7	1.38	290
NiO (700°C)	4.172	72.64	4.04	4.51	22	15.8	13.3	1.16	350
NiO (1100°C)	4170	27.58	20.4	31.7	56	37.4	22.3	2.67	460

Table 2.
Rietveld parameters of different NiO samples.

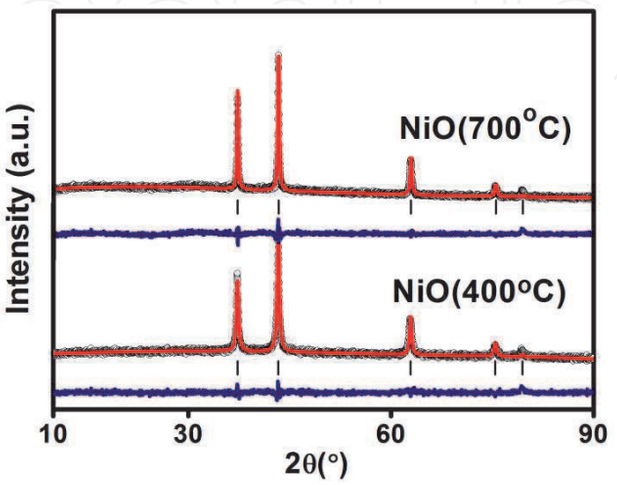


Figure 3.
Rietveld profile fit for NiO400 and NiO700 samples.

XRD patterns were profile-refined using the Full-Prof software package (http://www-llb.cea.fr/fullweb/). **Figure 3** gives the representative Rietveld profile fit for NiO400 and NiO700 samples along with different patterns obtained by using Fm3m (225) space group. The XRD analysis indicates that samples of nickel oxide have only one face-centered-cubic (fcc) phase. **Table 2** gives the parameters of samples found in the characterization. XRD study reveals all the peaks of NiO that are present, and the calculation indicates unit cell volume changes with stoichiometry.

5.2 Stoichiometry and defect analysis of nickel oxide

In nonstoichiometric compounds, there exist defects in the lattice structures of crystalline substances. As there are no absolute defect-free crystals at $T > 0$ K, hence these defects are related to nonstoichiometry. To determine oxygen content, that is, change in vacancy of nickel oxide formed by thermal decomposition method, the redox iodometric titration is the suitable method. For iodometric titration, standardized sodium thiosulfate and potassium iodide solution were used as a titrant and titrand, and starch solution is used as an endpoint indicator. The result obtained from iodometric titration was matched by the results of thermo-gravimetric analysis (TGA). The TGA system with the top of the line METTLER TOLEDO ultra-micro balance with unique built-in calibration weights ensures an accuracy of 0.1 mg was used.

For iodometric titrations, 0.0025 g sample was dissolved in KI and HCl solution. The concentration of KI was 0.1 mol^{-1} and concentration of HCl was ca. 0.1 mol^{-1}, titration was carried out using sodium thiosulfate (2.023×10^{-3} mol^{-1}) as a titrant. The starch solution was added prior to the end-point being reached as it acts as

indicator. **Table 1** shows the results of excess oxygen in NiO samples obtained by iodometric titration. The oxygen content of the samples indicates that the ratio of oxygen concentration to nickel concentration is greater than 1 for those samples, which were prepared below 700°C, and as the temperature increases above 700°C, the O/Ni ratio becomes nearly equal to 1.

The result of iodometric titration indicates that, on sintering, the precursor below 700°C nickel oxide having different oxygen contents can be prepared. As the sintering temperature is raised above 700°C, the excess oxygen present in the samples evolved, and the sample becomes stoichiometric. It can also be inferred from the above results that the oxidation state of nickel ions is also affected by sintering temperature. This titration also gives the amount of Ni^{3+} present in the samples, and hence the percentage of excess oxygen can also be determined. This can be obtained by considering that two Ni^{3+} ions correspond to three ions of O^{2-}.

The excess oxygen content of the samples was also calculated by TGA. The TGA analysis was performed in the inert atmosphere, in which the change in weight of a sample was analyzed with respect to temperature. TGA characterizes the materials according to its compositions. For our samples, by obtaining the weight loss with respect to increase in temperature, the weight of the excess oxygen is determined directly. **Figure 4a** gives the information about the thermogravimetric (TG) curve and its differential curve for NiO400 sample. Between 200 and 300°C, the sudden change in the mass of the sample is observed, and this indicates the amount of excess oxygen released in the heating process. This change in weight can also be associated with the desorption of oxygen from sample, which confirms nonstoichiometry. The other peak seen in the curve can be associated by the

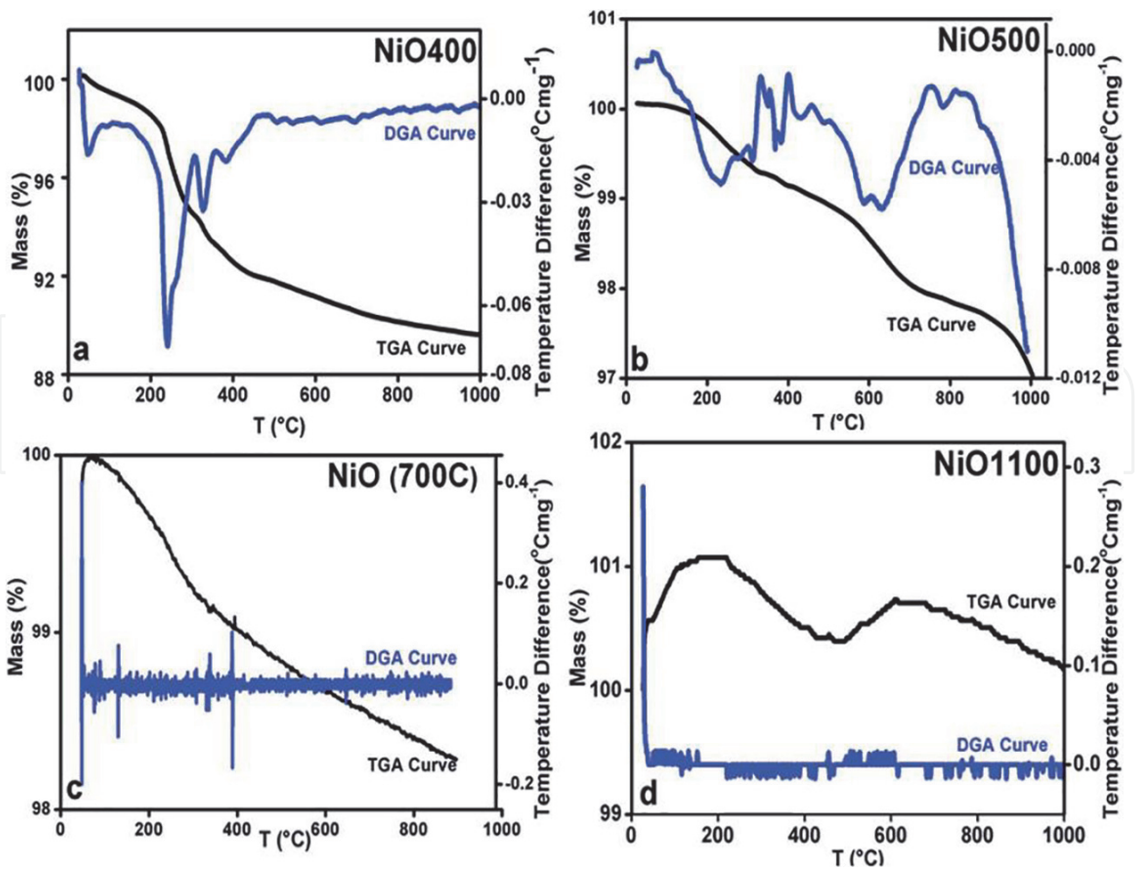


Figure 4.
TGA curves of nonstoichiometric $Ni_{1-\delta}O$ samples for (a) NiO400, (b) NiO500, (c) NiO700, and (d) NiO1100; heating rate of 5°C per min. The curves indicate the change in oxygen content of different samples as the sintering temperature increases.

evaporation of the physically bound water. Hence, this change in the weight does not have any contribution to the estimation of excess oxygen.

Unlike NiO400 TG and DGA curves for three more samples, that is, NiO500, NiO700, and NiO1100 were plotted and shown in **Figure 4b–d**. It is clear from the graphs that the loss in weight decreases as the sintering temperature for sample preparation increases. The change in mass for NiO500 sample is less than that of NiO400 sample and is negligible for the sample prepared above 700°C. The change in weight of samples directly indicates about excess oxygen present in the sample, which can be directly obtained from above TG curves and is shown in **Table 3**. Comparing the calculated excess oxygen in these nonstoichiometric samples by two different methods, it is understood that both results are similar to each other.

We have also prepared another sample of nickel oxide at 400°C, and the main difference is that this sample was prepared in the presence of oxygen. This sample is synthesized to understand the essential feature of excess oxygen in these nonstoichiometric samples. **Figure 5** shows the TG and DGA curves of this sample. The curves shown in **Figure 4a** and in **Figure 5** are almost similar. Hence, the samples of NiO400 prepared in air and in oxygen atmosphere are identical to each other. The weight of excess oxygen of sample prepared in presence of oxygen is slightly less as compared to NiO400 sample, which was prepared in air. The

Samples	Excess oxygen in iodometric titration (%)	Excess oxygen in thermogravimetric analysis (%)
NiO400	7.2	7.8 (6.4)*
NiO500	2.5	2.8
NiO600	1.4	1.6
NiO700	1.1	1.2
NiO800	0	0
NiO900	0	0
NiO1000	0	0
NiO1100	0	0

**% excess oxygen calculated for NiO400 sample prepared in presence of oxygen.*

Table 3.
Excess oxygen calculated from iodometric titration and TGA.

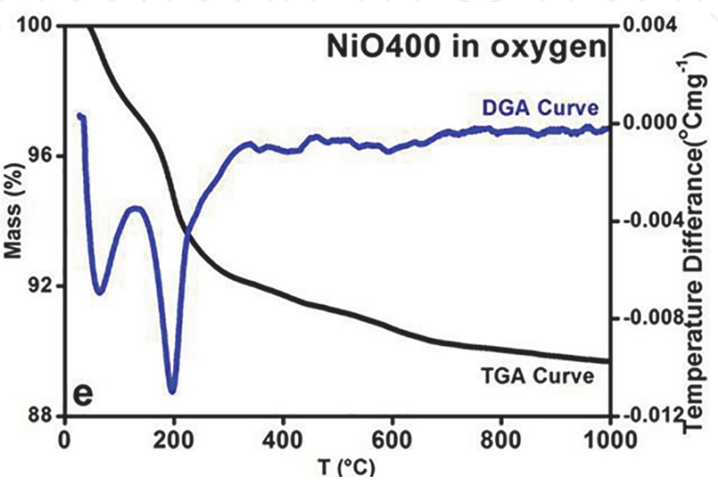


Figure 5.
TGA curve of NiO400 prepared in oxygen atmosphere.

difference in loss of weight percentage is calculated, and the values are reported in **Table 3**. Hence from iodometric and TGA analysis, it can be understood that due to rearrangement of atoms at high temperature, the defects of atoms get heals up and the sample that was nonstoichiometric at low temperature becomes stoichiometric. This is due to change in oxidation state with respect to change in temperature of sintering of precursor.

5.3 FTIR study of nonstoichiometric nickel oxide

FTIR spectroscopic study of $Ni_{1-\delta}O$ samples provides valuable information about the phase composition and the way in which oxygen is bonded to metal ions. **Figure 6a–d** show infrared (IR) transmission spectra of NiO400, NiO500, NiO700, and NiO1100 samples having different stoichiometry in the range between 400 and 4000 cm^{-1}. We observed a prominent peak in spectrum between 440 and 460 cm^{-1}. The slight shift in this peak for different samples is observed. This shift in the peak is noticed for all those samples that were sintered below 700°C. The reason of such peak shift can be attributed to stoichiometry of the samples. The observation of such peak in the long wavelength region, analogous to previous reports [26], could be assigned to the Ni–O stretching vibration mode, and the shifting is an indication of the nonstoichiometry present in these samples. In fact, in this long wavelength transverse optical mode, in which the sublattice of Ni^{2+} ions moves 180° opposite to the sublattice of O^{2-} ions for bulk NiO has been reported to lie between 390 and 405 cm^{-1} [27].

Some more peaks at 1032, 1383, and 1612 cm^{-1} in nonstoichiometric samples sintered below 700°C are seen prominently, which indicates the presence of hydroxide ions, nitrate ions, and some organic compounds. It is instructive to mention that the thermal analysis evidently identifies that the $Ni(NO_3)_2.6H_2O$ was decomposed completely to NiO at temperatures higher than 600°C [28]. The

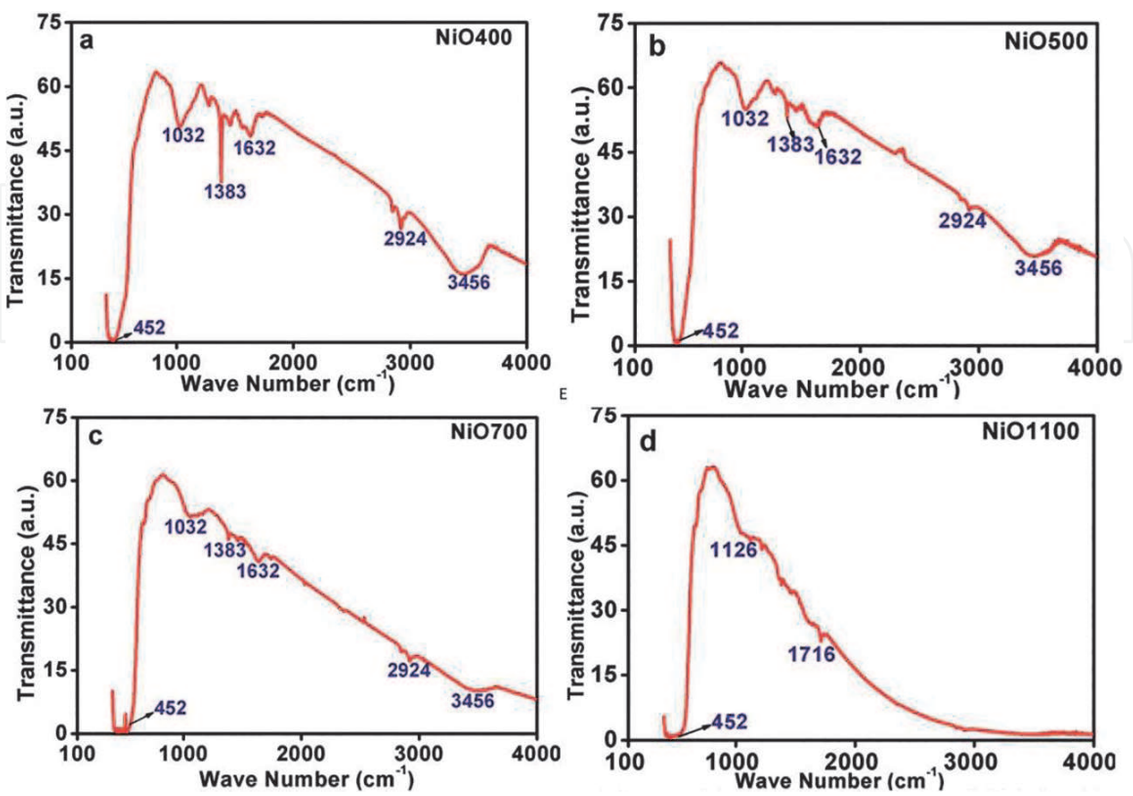


Figure 6.
FTIR of nonstoichiometric Ni1_dO samples for (a) NiO400, (b) NiO500, (c) NiO700, and (d) NiO1100.

samples that are sintered till 600°C may contain some organic molecules. Further, some of the bands found to be disappeared as the decomposition temperature increases as TGA data indict that at higher sintering temperature excess oxygen decreases [28]. Some carbon impurities are also present in the spectra, indicated by 2924 and 3456 cm^{-1} peaks in the spectrum. Hence, FTIR data shown in **Figure 6a–d**, TGA data shown in **Figure 4a–d**, and iodometric analysis data are corroborating each other and indicate that the samples are nonstoichiometric in nature. Analyzing the data obtained by the vacancy model, the concentration of hole in nickel oxide indicates that there is deficiency of metal in $Ni_{1-\delta}O$. Cationic vacancies of nickel in NiO are formed at nickel side due to the presence of excess oxygen. These vacancies can be ionized to create Ni^{3+} ions via the following reaction:

$$2Ni_{Ni}^{x} + \frac{1}{2}O_2 \rightarrow 2Ni_{Ni} + O_O^x + V_{Ni}'' \quad (1)$$

one ionized nickel vacancy (V_{Ni}'') and two Ni^{3+} ions ($Ni_{Ni}^{\cdot}$) will produce when two Ni^{2+} ions (Ni_{Ni}^{x}) will react with oxygen to produce in the NiO crystal. The holes are donated by each created Ni^{3+} ion, which also alters the conductive NiO. The results of iodometric titration, TGA, and FTIR analyses indicate that nonstoichiometric nickel oxide is nickel-deficient. Hence, nonstoichiometric nickel oxide behaves as p-type semiconductor because according to Eq. (1), we argue that an increase in number of nickel hole concentration increases as Ni^{3+} ions increase.

The majority of defects in nonstoichiometric nickel oxide is electron holes, which creates the vacancies. The vacancy model crated by holes is confirmed by a Seebeck coefficient [29], electrical conductivity [30], and other measurements. The kinetic measurements of the rate of oxidation of nickel metal to nickel oxide are also given by vacancy model [31]. The physical and chemical properties of nonstoichiometric nickel oxide are altered by the defect processes, and hence excess oxygen becomes prominent role player in such crystals.

By calculating inter atomic potentials, the energies of defect formation, migration, and substitution can be calculated by the atomistic simulation [32]. In the present case, the potential describing interionic interactions is represented by ionic pair-wise potentials of the form Eq. (2) Here, the first term represents long-range Coulomb, the second term corresponds to Hafemeister and Flygare form of short-range repulsive energies [33], and Van der Waals multipole are represented by third and fourth terms, respectively.

$$\phi(r) = \sum_{ij} \frac{Z_m e^2}{r_{ij}} + \sum_{ij} b\beta_{ij} \exp\left(\frac{r_i + r_j - r_{ij}}{\rho}\right) + \sum_{ij} c_{ij} r_{ij}^{-6} + \sum_{ij} d_{ij} r_{ij}^{-8}. \quad (2)$$

The symbols: c_{ij} and d_{ij} are the Van der Waals coefficients, and β_{ij} is the Pauling coefficient, respectively. Z_m is the modified ionic charge and parametrically includes the Coulomb screening effect, while b and r are short-range parameters. Thus, the effective interionic potential contains only three free parameters (Z_m, b, and r), which can be determined from the crystal properties [34]. The short-range potential parameters assigned to each ion-ion interaction were derived by empirical fitting to observed structural properties. In the context of the Columbic term, integral ionic charges are presumed, that is, 2^+ for Ni and 2^- for O, which enables a straight forward definition of hole states as Ni^{3+} or O^-. The deduced potential parameters are listed in **Table 4** for all the samples. It is clear from the calculated parameters as the sintering temperature of precursor increases, the nature of ordering in systems in which ions occupy sites on a face-centered-cubic (fcc) lattice

Samples	b (10^{-12} erg)	P (Å)	F (eV)
NiO400	39.51	0.388	39.592
NiO500	39.46	0.388	39.602
NiO600	39.40	0.388	39.612
NiO700	39.38	0.388	39.623
NiO800	39.40	0.388	39.612
NiO900	39.41	0.388	39.612
NiO1000	39.57	0.388	39.518
NiO1100	39.41	0.388	39.612

Table 4.
Interatomic potential parameter of nickel oxide sintered at different temperatures as discussed in Eq. (2).

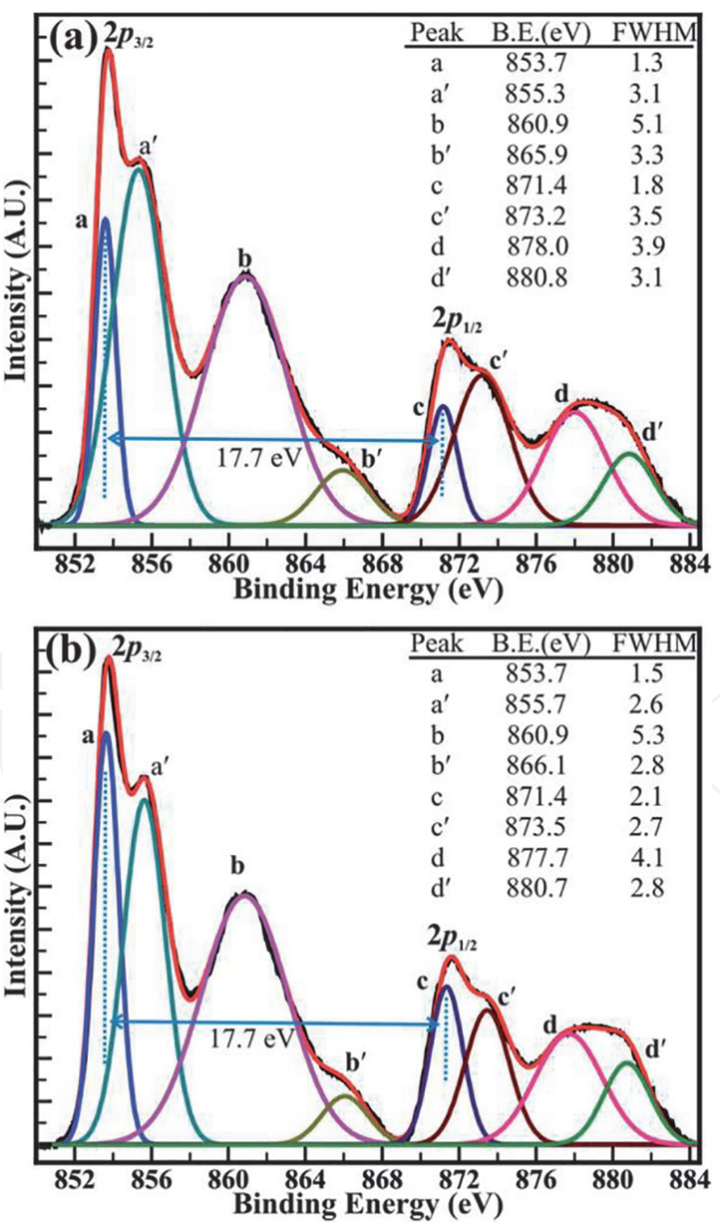


Figure 7.
High-resolution XPS spectra of the Ni (2p) core levels of the Ni oxides decomposed at a temperature of (a) 500° C and (b) 700°C. The XPS spectra were decomposed using Voigt peak function fittings.

changes and the nearest-neighbor (NN) and next-nearest neighbor (NNN) exchange interactions also get altered. This happens in such a manner that the structure of NiO undergoes a week cubic-to-rhombohedral distortion as a result of the magnetostriction effect in the presence of excess oxygen in the samples [35]. The NN and NNN exchange interactions and the antiferromagnetic (AFM) structure of NiO are altered due to the presence of excess oxygen in the samples. Since the radius of Ni^{3+} ions is smaller than that of Ni^{2+}. The Ni^{3+}-O^{2-} bond distance will be short for those samples whose oxygen content is higher. In due course, interatomic potential parameters and bond length change as the sintering temperature changes, the magnetic ordering transition temperature is expected to change as we will discuss in later sections.

5.4 XPS studies of nonstoichiometric nickel oxide

The chemical properties and stoichiometry of nickel oxide were studied by XPS analysis. For NiO500 and NiO700, XPS spectra of Ni (2p) core level are shown in **Figure 7a** and **b**, while the XPS spectra for NiO400 and NiO1100 are shown in **Figure 8**.

In both the spectra, distinct peaks for different binding energies can be observed clearly along with the double peak features. These double peak features represented for the Ni (2p) core levels are observed in all samples. Voigt peak fitting function is used to analyze the double peak features of Ni($2p_{3/2}$) and Ni($2p_{1/2}$). These peaks were fitted within the Shirley background. The binding energy of 853.7 (±0.2), 855.5 (±0.2), 860.6 (±0.2), 865.9 (±0.2), 871.4 (±0.2), 873.3 (±0.2), 877.9 (±0.2), and 880.7 (±0.2) eV represented by a, a′, b, b′, c, c′, d, and d′ are associated with all eight peaks, which are perfectly fit. The peaks marked as a, a′, c, and c′, represent core levels of $Ni^{2+}(2p_{3/2})$, $Ni^{3+}(2p_{3/2})$, $Ni^{2+}(2p_{1/2})$, and $Ni^{3+}(2p_{1/2})$, respectively. The decomposed shake-up satellite peaks (marked as b, b′, d, and d′) were observed at ~7.1(±0.2) or 10.2(±0.2) eV and ~6.3(±0.3) or ~7.1(±0.2) eV higher in binding energy than that of $Ni^{2+}(2p_{3/2})$, $Ni^{3+}(2p_{3/2})$, $Ni^{2+}(2p_{1/2})$, and $Ni^{3+}(2p_{1/2})$ peaks, respectively. The magnetic chemical state of Ni^{2+} and Ni^{3+} ions can be associated with the double peak features of Ni(2p). The consecutive shake-up satellite peaks also give information of the same [36]. The positions of the XPS peaks obtained in different nonstoichiometric samples are analogs to previous studies [37]. The O(1 s) XPS spectra of the samples obtained were similar to each other. **Figure 8** shows the O(1 s) spectra Voigt peak fitting function within the Shirley background. The binding energy of 529.3 and 531.1 eV with FWHM of 1.2 and 1.7 eV are clearly observed in the figure for oxygen spectra. Hence, two peaks are clearly obtained for O(1 s) spectra. The lower binding energy peak observed at 529.3 eV corresponds to the O(1 s) core level of O^{2-} anions associated with Ni-O chemical bonding. However, higher binding energy peak observed at 531.1 represents the surface contamination or presence of hydroxyl (−OH) groups [37].

The close analysis of decomposed XPS spectrum revealed that the intensity of the peaks assigned to core levels of $Ni^{3+}(2p_{3/2})$ and $Ni^{3+}(2p_{1/2})$ is larger than that of core levels $Ni^{2+}(2p_{3/2})$ and $Ni^{2+}(2p_{1/2})$ at decomposition temperature of 400 and 500°C. However, the intensity of the peaks of $Ni^{2+}(2p_{3/2})$ and $Ni^{2+}(2p_{1/2})$ core levels has increased than that of the peaks of $Ni^{3+}(2p_{3/2})$ and $Ni^{3+}(2p_{1/2})$ core levels after the decomposition temperature of 700°C and is continued to increase for the temperature of 1100°C. The intensity ratio obtained for the peaks of the $Ni^{2+}(2p_{3/2})$ and $Ni^{3+}(2p_{3/2})$ core levels (i.e., Ni^{2+}/Ni^{3+}) has increased from 0.85 (±0.03) to 1.23 (±0.03) with an increase in the temperature from 400 to 1100°C.

It is evident that for the samples prepared at 500 and 700°C have more prominent variation of intensity, and hence the Ni^{2+} and Ni^{3+} are more easily bifurcated at

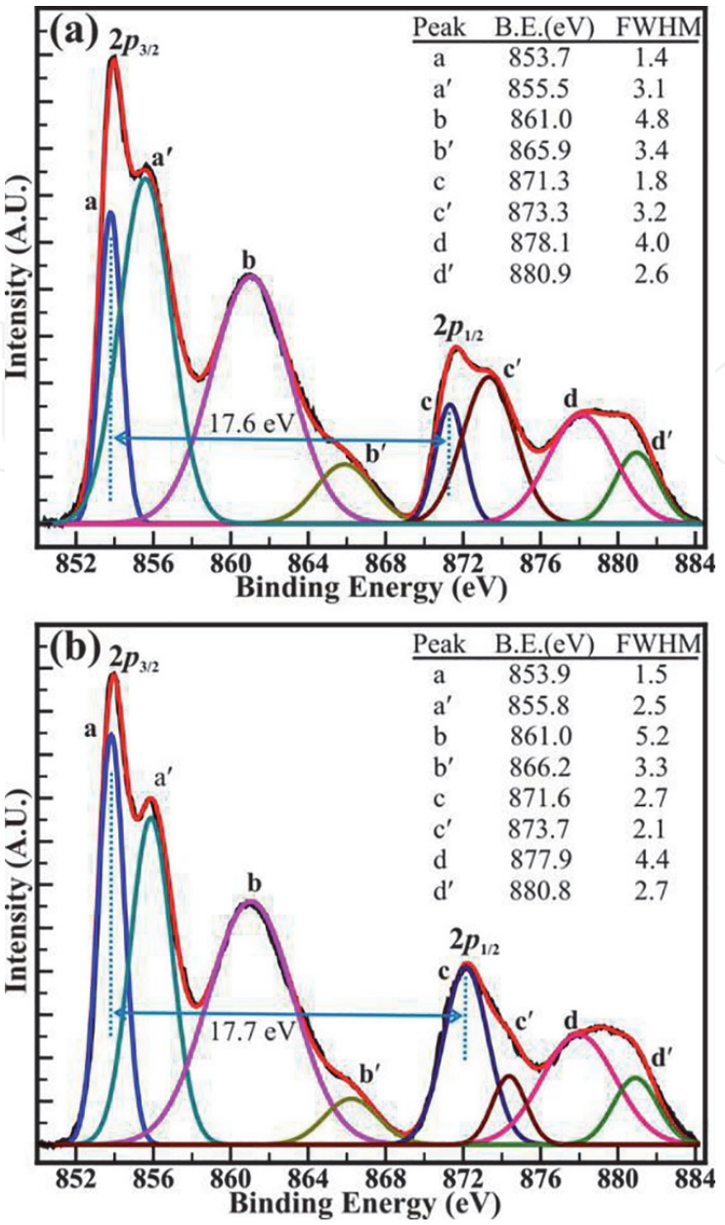


Figure 8.
High-resolution XPS spectra of the Ni (2p) core levels of the Ni oxides decomposed at a temperature of (a) 400° C and (b) 700°C. The XPS spectra were decomposed using Voigt peak function fittings.

these temperatures because the conversion of Ni^{3+} ions into Ni^{2+} ions is fast. And the binding energy difference (ΔE) of 17.7 (±0.1) eV between the Ni($2p_{3/2}$) and Ni ($2p_{1/2}$) peaks is very close to that of 17.8 eV for oxidized Ni and significantly larger than that of 17.2 eV for metallic Ni [38]. Hence, all the nickel is converted into oxide form, and there is no nickel present in the metal form. This can be confirmed by XPS investigation that the nonstoichiometric NiO400 contains Ni^{3+} ions in higher quantity as compared to NiO1000. The XPS analysis also corroborates with our TGA analysis for nonstoichiometric nickel oxide. Hence, the oxygen content of the samples can be controlled by controlling the temperature of preparation of samples. Hence, nonstoichiometry in nickel oxide can be created by controlling temperature of preparation.

5.5 Magnetic properties measurements of nonstoichiometric nickel oxide

The magnetic characterization of nonstoichiometric samples was performed to obtain the magnetic susceptibility (χ). These measurements were done for selected

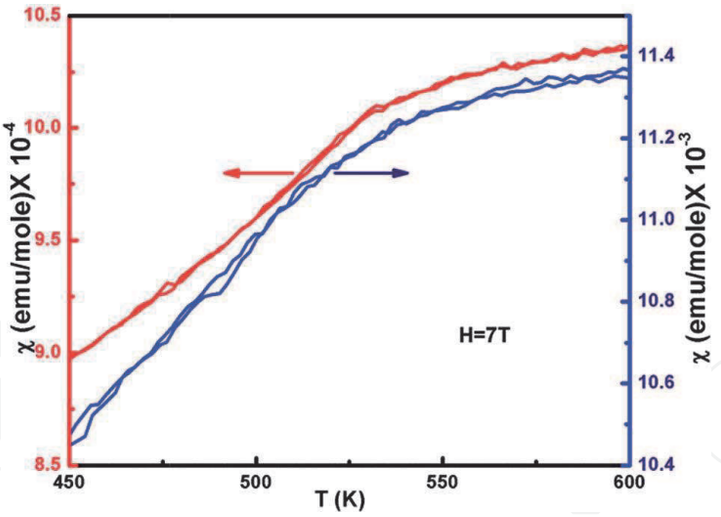


Figure 9.
Magnetization for ZFC and FC curves of nonstoichiometric $Ni_{1-\delta}O$ samples for NiO400 and NiO1100 in 7 T applied field as a function of temperature.

samples of NiO400 and NiO1100. Temperature-dependent magnetic susceptibility (χ) is shown in **Figure 9**. This measurement was performed at an applied magnetic field of 7 Tesla. Both zero-field-cooled (ZFC) and field-cooled (FC) conditions were employed to measure the susceptibility (χ) of nonstoichiometric nickel oxide samples. We observed a reversible behavior with negligible hysteresis of χ for different stoichiometry. It is interesting to describe that sample shows paramagnetic (PM) to antiferromagnetic (AFM) transition. This transition is observed at the Néel temperature T_N. But the transition temperature at which transition takes place is different in both the samples. The values are 480 and 530 K for NiO400 and NiO1100 samples, respectively. T_N and the absolute value of χ for NiO400 sample are lower than that of NiO1100 sample. However, PM to AFM transition width appears to be broader for the NiO1100 sample. This can be understood as T_N changes with stoichiometry, which could be attributed to the effect of the partial destruction of Ni^{2+}–O–Ni^{3+} exchange interaction network because of the reduction of the oxygen vacancies and the weakening of Ni^{2+}–O–Ni^{3+} interaction arising from the decrease of the bandwidth of, for example, electrons due to the change in Ni–O bond length and Ni–O–Ni bond angle [39].

5.6 Specific heat measurement

Figure 10 shows the change in specific heat with respect to temperature of nonstoichiometric NiO. The irregularity or the change in specific heat for different samples is found in the vicinity of T_N. This shows that AFM ordering of these samples is affected by oxygen content of the samples. A shift in anomaly is probed as the stoichiometry of sample changes. Change in heat capacity of different samples, due to stoichiometry, also alters the transition temperature. Hence, as the sintering temperature increases, T_N will change and finally attain a fixed value. It is observed from the heat capacity graph that the transition temperature for NiO500, NiO700, and NiO1100 samples are 510, 519, and 525 K, respectively. It is understood that due to excess oxygen in the different ratios in NiO400 and NiO500 samples, change in specific heat anomaly is observed. Further, the observed transition temperature reaches to 525 K as reported for stoichiometric NiO [40]. An irregular behavior in Cp at T_N is due to Ni-spin ordering as suggested by Néel [41] wherein due to the thermal agitation spin-lattice of the particle could reverse coherently and randomly.

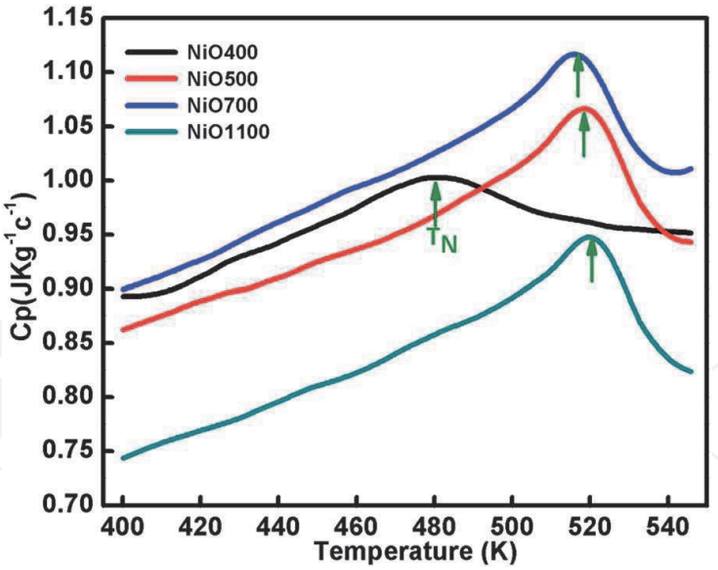


Figure 10.
The temperature variation of specific capacity of nickel oxide samples sintered at different temperatures. Curve shows shifting in TN due to different oxygen contents of the samples.

Consequently, the net moment of uncompensated surface spins would fluctuate accordingly and in turn, significant downshift the T_N in samples due to both the change of magnetic ions as well as their disorder. Probably due to change in excess oxygen, magnetic inhomogeneity in nonstoichiometric samples increases, and Néel temperatures eventually shift.

6. Conclusion

The samples of different oxygen contents of nickel oxide were synthesized by thermal decomposition method. The structure of these samples was characterized by X-ray diffraction spectroscopy, and full-proof refinement was used for indexing. The nonstoichiometry of these samples was recognized by iodometric titration and thermogravimetric analysis. Both these techniques give the excess oxygen content of samples, which was found to be similar. Different phases of nickel oxide were confirmed by the FTIR studies. The shift in FTIR pattern indicates about the nonstoichiometry of samples. The change in stoichiometry of sample is also responsible for the defect creation in the samples, as XPS results indicate that nickel vacancy can be created in samples with varying sintering temperatures. Those samples that were sintered at low temperature have high defect as compared to sample sintered at high temperature. The ZFC and FC curves are nearly identical to each other but the susceptibility changes with stoichiometry. The observed specific heat anomaly in the vicinity of T_N is associated with the magnetic ordering, indicating a gradual transformation between two magnetic phases, and the observed T_N shifted toward lower temperatures as excess oxygen content increases. The shifting of Néel temperature is presumably due to magnetic inhomogeneity arising from the excess oxygen in samples.

Acknowledgements

The authors would like to thank Dr. A. M. Awasti, Dr. Mukul Gupta, and Dr. V. Ganesan, Centre Director, UGC-DAE-CSR, Indore, India for providing heat

capacity measurements and XRD facilities. Financial support from the Science and Engineering Research Board (SERB), the Department of Science and Technology (DST), New Delhi, and the Madhya Pradesh Council of Science and Technology (MPCST), Bhopal (NK) are gratefully acknowledged.

Conflict of interest

The authors declare that there are no conflicts of interest.

Author details

Paras Dubey[1] and Netram Kaurav[2*]

1 Department of Physics, Institute of Sciences, SAGE University, Indore, Madhya Pradesh, India

2 Department of Physics, Government Holkar Science College, Indore, Madhya Pradesh, India

*Address all correspondence to: kauravnetram@gmail.com; netramkaurav@yahoo.co.uk

IntechOpen

© 2019 The Author(s). Licensee IntechOpen. This chapter is distributed under the terms of the Creative Commons Attribution License (http://creativecommons.org/licenses/by/3.0), which permits unrestricted use, distribution, and reproduction in any medium, provided the original work is properly cited. CC BY

References

[1] Kim YS, Kim J, Yoon MJ, Sohn CH, Lee SB, Lee D, et al. Impact of vacancy clusters on characteristic resistance change of nonstoichiometric strontium titanate nano-film. Applied Physics Letters. 2014;**104**: 013501-1-5. DOI: 10.1063/1.4955268

[2] Huang S, Ou G, Cheng J, Li H, Pan W. Ultrasensitive visible light photoresponse and electrical transportation properties of nonstoichiometric indium oxide nanowire arrays by electrospinning. Journal of Materials Chemistry C. 2013; **1**:6463-6470. DOI: 10.1039/C3TC31051E

[3] Yang Y, Liu XL, Yang Y, Xiao W, Li ZW, Xue DS, et al. Synthesis of nonstoichiometric zinc ferrite nanoparticles with extraordinary room temperature magnetism and their diverse applications. Journal of Materials Chemistry C. 2013;**1**: 2875-2885. DOI: 10.1039/C3TC00790A

[4] Fergus JW. Oxide materials for high temperature thermoelectric energy conversion. The Journal of the European Ceramic Society. 2012;**32**:525-540. DOI: 10.1016/j.jeurceramsoc.2011.10.007

[5] Lipatnikov VN, Zueva LV, Gusev AI, Kottar A. Disorder-order phase transformations and electrical resistivity of nonstoichiometric titanium carbide. Physics of the Solid State. 1998;**40**: 1211-1218. DOI: 10.1134/1.1130523

[6] Gusev AI. Order-disorder transformations and phase equilibria in strongly nonstoichiometric compounds. Uspekhi Fizicheskikh Nauk. 2003;**170**: 3-40. DOI: 10.3367/UFNr.0170. 200001a.0003

[7] Sugiyma I, Shibata N, Wang Z, Kobayashi S, Yamamoto T, Ikuhara Y. Ferromagnetic dislocations in antiferromagnetic NiO. Nature Nanotechnology. 2013;**8**:266-270. DOI: 10.1038/nnano.2013.45

[8] Sato H, Minami T, Takata S, Yamada T. Transparent conducting p-type NiO thin films prepared by magnetron sputtering. Thin Solid Films. 1993;**236**:27-31. DOI: 10.1016/ 0040-6090(93)90636-4

[9] Hotovy I, Huran J, Spiess L, Hascik S, Rehacek V. Preparation of nickel oxide thin films for gas sensors applications. Sensors and Actuators, B: Chemical. 1999;**57**:147-152. DOI: 10.1016/ S0925-4005(99)00077-5

[10] Shima H, Takano F, Akinaga H. Resistance switching in the metal deficient-type oxides: NiO and CoO. Applied Physics Letters. 2007;**91**: 012901. DOI: 10.1063/1.2753101

[11] Sun YK, Myung ST, Park BC, Prakash J, Belharouak I, Amine K. High-energy cathode material for long-life and safe lithium batteries. Nature. 2009; **8**:320-324. DOI: 10.1038/nmat2418

[12] Caruge J, Halpert JE, Bulovic V, Bawendi MG. NiO as an inorganic hole-transporting layer in quantum-dot light-emitting devices. Nano Letters. 2006;**6**: 2991-2994. DOI: 10.1021/nl0623208

[13] Ferrari AM, Pisani C, Cinquini F, Giordano L, Pacchioni G. Cationic and anionic vacancies on the NiO(100) surface: DFT+UDFT+U and hybrid functional density functional theory calculations. The Journal of Chemical Physics. 2007;**127**:174711-174716. DOI: 10.1063/1.2796154

[14] Nowotny J, Sadowski A. Application of microcalorimetry in studies of interaction between oxygen and NiO single crystals. Journal of the American Ceramic Society. 1979;**62**:241-253. DOI: 10.1007/BF00656843

[15] Kofstad P. Nonstoichiometry, Diffusion, and Electrical Conductivity in Binary Metal Oxides. New York: Wiley; 1972. DOI: 10.1007/BF01046721

[16] Conell RS, Corrigan DA, Powell BR. The electrochromic properties of sputtered nickel oxide films. Solar Energy Materials and Solar Cells. 1992; **25**:301-313. DOI: 10.1016/0927-0248(92)90075-Z

[17] Patil PS, Kadam DS. Preparation and characterization of spray pyrolyzed nickel oxide (NiO) thin films. Applied Surface Science. 2002;**199**:211-221. DOI: 10.1016/S0169-4332(02)00839-5

[18] Iida Y, Kenjo S, Ozaki S. Non-stoichiometry of nickel oxide. Bulletin of the Chemical Society of Japan. 1960; **33**:1372-1375. DOI: 10.1246/bcsj.33.1372

[19] Chen HL, Lu YM, Hwang WS. Effect of film thickness on structural and electrical properties of sputter-deposited nickel oxide films. Materials Transactions. 2005;**46**:872-879. DOI: 10.2320/matertrans.46.872

[20] Kodama RH, Makhlouf SA, Berkowitz AE. Finite size effects in antiferromagnetic NiO nanoparticles. Physical Review Letters. 1997;**79**: 1393-1399. DOI: /10.1103/PhysRevLett.79.1393

[21] Pramanik P, Bhattachraya S. A chemical method for the deposition of nickel oxide thin films. Journal of the Electrochemical Society. 1990;**137**:3869-3870. DOI: 10.1149/1.2086316

[22] Lampert CM, Omstead TR, Tu PC. Chemical and optical properties of electrochromic nickel oxide films. Solar Energy Materials. 1986;**14**:161. DOI: 10.1016/0165-1633(86)90043-2

[23] Surca A, Orel B, Pilhar B, Bwkovec P. Optical, spectroelectrochemical and structural properties of sol-gel derived Ni-oxide electrochromic film. The Journal of Electroanalytical Chemistry. 1996;**408**: 83-100. DOI: 10.1016/0022-0728(96)04509-3

[24] Kim KS, Winograd N. X-ray photoelectron spectroscopic studies of nickel-oxygen surfaces using oxygen and argon ion-bombardment. Surface Science. 1974;**43**:625-643. DOI: 10.1016/0039-6028(74)90281-7

[25] Brockner W, Ehrhardt C, Gjikaj M. Thermal decomposition of nickel nitrate hexahydrate, $Ni(NO_3)_2{\cdot}6H_2O$, in comparison to $Co(NO_3)_2{\cdot}6H_2O$ and $Ca(NO_3)_2{\cdot}4H_2O$. Thermochimica Acta. 2007;**456**:64-68. DOI: 10.1016/j.tca.2007.01.031

[26] Yu C, Nazri G, Lampert CM. Spectroscopic and electrochemical studies of electrochromic hydrated nickel oxide films. Solar Energy Materials. 1987;**16**:1-17. DOI: 10.1016/0165-1633(87)90003-7

[27] Nakagawa I. Far-infrared reflection spectra, optical and dielectric constants, and lattice vibrations of some fluoride crystals. Bulletin of the Chemical Society of Japan. 1971;**44**:3014-3020. DOI: 10.1246/bcsj.44.3014

[28] Moore WJ. Seven Solid States. W. A. WA, USA: Benjamin, Inc; 1967

[29] Bosman AJ, Daal HJ, Van GF, Knuvers GF. Hall effect between 300° K and 1100° K in NiO. Physics Letters. 1965;**19**:372-373. DOI: 10.1016/0031-9163(65)90901-7

[30] Osburn CM, Vest RW. Defect structure and electrical properties of NiO—I. high temperature. Journal of Physics and Chemistry of Solids. 1971; **32**:1331-1342. DOI: 10.1016/S0022-3697(71)80191-9

[31] Fueki K, Wegner JB. Studies of the oxidation of nickel in the temperature range of 900° to 1400°C. Journal of the Electrochemical Society. 1965;**112**: 384-388. DOI: 10.1149/1.2423553

[32] Catlow CRA. Computer simulation studies of transport in solids. Annual Review of Materials Science. 1986;**16**: 517-548. DOI: 10.1146/annurev.ms.16.080186.002505

[33] Hafemeister DW, Flygare WH. Outer-Shell overlap integrals as a function of distance for halogen—Halogen, halogen—Alkali, and alkali—Alkali ions in the alkali halide lattices. The Journal of Chemical Physics. 1965; **43**:795. DOI: 10.1063/1.1696846

[34] Kaurav N. High-pressure phase transformation and elastic behavior of XC (X = Si, Ge, Sn and Pt) compounds. Physica Scripta. 2013;**88**: 015604-015609. DOI: 10.1088/0031-8949/88/01/015604

[35] Mironova-Ulmane N, Skvortsova V, Kuzmin A. Magnetic ion exchange interactions in NiO-MgO solid solutions. Physics of the Solid State. 2005;**47**: 1516-1522. DOI: 10.1134/1.2014504

[36] Shaikh JS, Pawar RC, Devan RS, Ma YR, Salvi PP, Kolekar SS, et al. Synthesis and characterization of Ru doped CuO thin films for supercapacitor based on Bronsted acidic ionic liquid. Electrochimica Acta. 2011;**56**:2127-2134. DOI: 10.1016/j.electacta.2010.11.046

[37] Wagner CD, Riggs WM, Davis LE, Moulder JF, Muilenberg GE. Handbook of X-Ray Photoelectron Spectroscopy. Minnesota: Perkin-Elmer Corporation; 1979. DOI: 10.1002/sia.740030412

[38] Devan RS, Lin C-L, Gao S-Y, Cheng C-L, Liou Y, Ma Y-R. Room-temperature wide-range photoluminescence and semiconducting characteristics of two-dimensional pure metallic Zn nanoplates. RSC Advances. 2012;**2**:2123-2127. DOI: 10.1039/C2RA00972B

[39] Lenglet M, Hochu F, Durr J, Tuilier MH. Investigation of the chemical bonding in $3d^8$ nickel(II) charge transfer insulators (NiO, oxidic spinels) from ligand-field spectroscopy, Ni 2*p* XPS and X-ray absorption spectroscopy. Solid State Communications. 1997;**104**:793-798. DOI: 10.1016/S0038-1098(97)00273-1

[40] Hutchings MT, Samuelsen EJ. Measurement of spin-wave dispersion in NiO by inelastic neutron scattering and its relation to magnetic properties. Physical Review B. 1972;**6**:3447-3456. DOI: 10.1103/PhysRevB.6.3447

[41] N'eel L. Superposition de l'antiferromagnétisme et du superparamagnétisme dans un grain très fin. Comptes Rendus de l'Académie des Sciences. 1961;**252**:4075-4079